

The pressure dependence of electron-phonon coupling in the organic superconductor κ -(BEDT-TTF)₂Cu(SCN)₂: A comparison of high pressure infrared reflectivity and Raman scattering experiments.

R. D. McDonald, A-K. Klehe, J. Singleton and W. Hayes

Clarendon Laboratory, Department of Physics, Parks Road, Oxford, OX1 3PU, UK.

(Dated: May 2001)

We determine the pressure dependence of the electron-phonon coupling constant in κ -(BEDT-TTF)₂Cu(SCN)₂ by comparison of high pressure Raman scattering and high pressure infrared reflectivity (IR) measurements. We use comparison of the IR reflection spectrum from deuterated and protonated samples to aid the deconvolution of several overlapping phonon modes. These coupled modes are modelled with a Green's function to extract the linear pressure dependence of the individual modes. The Raman active molecular vibrations of the BEDT-TTF dimers stiffen by 0.1-1 %GPa⁻¹. In contrast, the corresponding modes in the IR spectrum are observed at lower frequency, with a pressure dependence of 0.5-5.5 %GPa⁻¹, due to the influence of the electron-phonon interaction. The stronger pressure dependence of the central C=C mode of the BEDT-TTF molecule in the IR, is discussed. Our analysis suggests that reduction of electron-phonon coupling under pressure does not account for observed suppression of superconductivity under pressure.

κ -(BEDT-TTF)₂Cu(SCN)₂ is one of the best characterized organic superconductors [1]. It is a highly anisotropic material with a quasi-two dimensional band structure, whose Fermi-surface topology has been determined by magnetotransport experiments [1, 2]. At ambient pressure κ -(BEDT-TTF)₂Cu(SCN)₂ is a superconductor with a transition temperature of $T_c \simeq 10.4$ K. T_c decreases upon the application of pressure until, at pressures P exceeding 0.5 GPa, superconductivity is fully suppressed [2, 3]. The effective mass, m^* , derived from magnetic quantum oscillation measurements, decreases linearly with pressure up to 0.5 GPa; above this pressure the magnitude of dm^*/dP is strongly reduced [2]. In contrast, the effective mass derived from optical measurements, m_{opt} , decreases approximately linearly throughout this pressure range [4]. The coincidence of a "kink" in the pressure dependence of m^* with the pressure above which superconductivity is suppressed and the absence of a "kink" in the pressure dependence of m_{opt} , indicates that the interactions parameterised by m^* are connected to the superconductivity.

The key question to address is the effect of these interactions, *i.e.* what is the dominant pairing mechanism for superconductivity in this material? In this paper we compare infrared (IR) [4] and Raman scattering [5] measurements under pressure to determine the role of the electron-phonon interaction. This is possible because the IR measurement probes the molecular vibrations dressed by the electron-phonon interaction [6, 7], whereas non-resonant Raman measurements probe the bare mode frequencies [7, 8]. Our recent high-pressure IR study [4] of this material revealed anomalously large mode stiffening for the molecular vibrations most strongly coupled to the electronic excitations. However, determination of the pressure dependence of the most strongly coupled mode, at around 1300 cm⁻¹ in the IR spectrum, is not straightforward due to the mixing of several modes with varying pressure dependence. In the current paper we use the comparison of ambient pressure reflectance data

from protonated and deuterated samples to establish a coupled oscillator model. This model is then employed to determine pressure induced frequency shifts of the interacting modes. By employing a dimer charge-oscillation model [7, 8, 9], comparison of the pressure induced frequency shifts observed in both the IR [4] and the Raman [5] spectra determines the pressure dependence of the electron-phonon interaction. Four modes are observable in both the high-pressure Raman and IR spectra (see Table II). They are labeled with subscripts indicating the atoms/bond predominantly involved in the vibration [10]. In order of increasing frequency they are: the C-S mode originating from the BEDT-TTF 60 B_{3g} asymmetric vibration, the central C=C mode originating from the BEDT-TTF 3 A_g symmetric vibration and two Cu(SCN)₂ anion modes.

Owing to its strong electron-phonon coupling [7], we are particularly interested in extracting the pressure induced frequency shift of the central C=C mode. Dimerization in the κ -phase makes this mode IR active [7, 11]. Electron-phonon coupling softens this mode from its bare, Raman active, frequency of 1470 cm⁻¹ to around 1290 cm⁻¹ along the *b*-axis and around 1220 cm⁻¹ along the *c*-axis. This brings the mode into resonance with the end carbon-hydrogen (C-H) oscillations of the BEDT-TTF molecule [12]. Upon deuteration the C-H(D) modes are softened sufficiently to reveal the true line shape of the central C=C mode. Comparison of the IR spectrum from the protonated and deuterated salts illustrates the structure of the C=C mode due to this coupling (see Fig. 1b and 1d); dips occur where the stronger C=C mode loses spectral weight to the weaker C-H modes it is driving.

Although mode mixing should be treated from a quantum mechanical point of view, it has been shown [13] that a classical approach, such as described below, can yield information regarding the individual mode frequencies. From the equations of motion (Fourier components) for a set of N coupled oscillators [14], a Green's-function

matrix approach [15] is employed to model the dielectric response function

$$\epsilon(\omega) = \Omega_p \{G(\omega)\}^{-1} \Omega_p^T, \quad (1)$$

where Ω_p is a vector containing each oscillator's spectral weight, Ω_p^T is its transpose and G is a square matrix of dimension N , with N the number of oscillators. The diagonal terms in G are of the form

$$G_{aa}(\omega) = (\omega_a^2 + i\omega\Gamma_a - \omega^2), \quad (2)$$

specifying each Lorentzian oscillator of frequency ω_a and damping Γ_a . The off-diagonal terms in G provide the coupling and are of the form

$$G_{ab}(\omega) = (\Delta_{ab}^2 + i\omega\Gamma_{ab}). \quad (3)$$

This coupled oscillator model is employed to analyze our room temperature high-pressure IR reflectance [4]. The aim is to extract the pressure-induced frequency shift of individual modes from the apparently non-linear shift (predominantly in the c -axis response) of the reflectance peaks as a function of pressure (the crosses in Fig. 1a and Fig. 1c).

To restrict the possible parameter space encountered, a simple (uncoupled) Drude-Lorentz oscillator fit to the ambient-pressure room-temperature IR spectrum of the deuterated salt was used as a starting point, (the dotted line in figure 1b and 1d). In the absence of coupling the asymmetric line shape of the central C=C mode for both b and c axes is most accurately reproduced when the Drude term is heavily suppressed, *i.e.* damped to the point that it hardly contributes to the reflectance in this frequency range. The terms describing the background and C=C mode were then held fixed and free parameters describing the two C-H modes and their coupling terms were introduced. A least squares fitting procedure was employed, yielding the parameters necessary to model the interacting modes in the protonated salt at room temperature and ambient pressure (the dashed and solid line in figures 1b and 1d respectively).

For both b - and c -axis polarizations and both the protonated and deuterated samples the damping and strength of the two C-H(D) modes tended to the same values, $\Gamma_{H(D)} \rightarrow 16 \text{ cm}^{-1}$ and $\Omega_{p,H(D)} \rightarrow 0$, *i.e.* two sharp modes with no infrared activity of their own. The coupling strengths, Δ (see equ.(3)), are listed in table I, with the cross damping term Γ_{ab} also tending to zero for all modes. With all parameters except the three

Parameter	b-axis value cm^{-1}	c-axis value cm^{-1}
$\Delta_{\text{CC,CH}_1}$	260	230
$\Delta_{\text{CC,CH}_2}$	260	230
$\Delta_{\text{CH}_1,\text{CH}_2}$	160	0

TABLE I: mode coupling parameters.

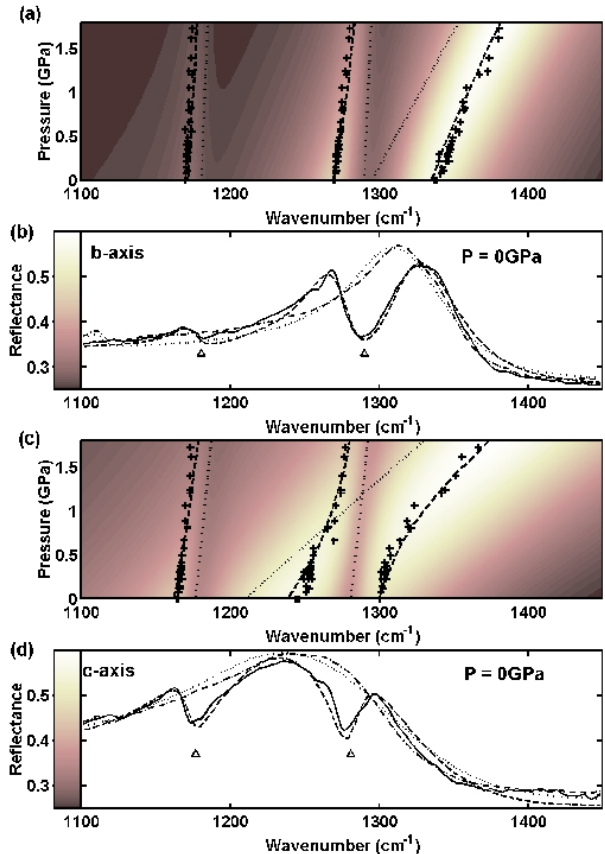


FIG. 1: (a) and (c) diamond/sample reflection surfaces generated from the coupled oscillator model for the b and c axis respectively; the reflectance scales are adjacent to the vertical axes of (b) and (d). Superimposed are the frequency of reflectance peaks (crosses) [4], uncoupled mode frequencies (dotted lines) and the peaks of the coupled oscillator model (dashed lines). (b) and (d) The ambient pressure reflection spectrum for polarization parallel to the b and c axes respectively: solid and dashed lines for the protonated salt (measurement and fit), dash-dot and dotted lines for the deuterated salt (measurement and fit).

mode frequencies held constant, the pressure-induced frequency shifts of the reflectance peaks were fitted. The data could be successfully modelled with only first order (linear) pressure shifts included (see Fig. 1a and 1c and table II).

Including a pressure-dependent Drude response to account for the increase in background reflectance in this spectral region has a small effect ($\approx +0.5\%$) on the observed peak frequencies in the reflectance model. Its main effect is to broaden and distort the line shape of the phonon modes towards higher frequency, as experimentally observed at high pressure [4].

Within the framework of a dimer charge oscillation model [8] it is possible to calculate a dimensionless electron-phonon coupling constant, λ , using a mode's IR frequency, ω_{IR} , and the corresponding Raman frequency, ω_{R} , given knowledge (see Table II) of the energy, ω_{CT} , of

Mode	Raman cm ⁻¹ +(%GPa ⁻¹)	Infrared b-axis cm ⁻¹ +(%GPa ⁻¹)	Infrared c-axis cm ⁻¹ +(%GPa ⁻¹)
ω_{CT}	—	2910 + 4.0	2390 + 4.0
ω_{CS}	886.2 + 0.85	883.5 + 0.71	873.6 + 1.0
ω_{CC}	1467.7 + 0.4	1290 + 2.5	1210 + 5.5
ω_{CH_1}	—	1181 + 0.5	1177 + 0.5
ω_{CH_2}	—	1290 + 0.5	1281 + 0.5
ω_{CD_1}	—	1027 †	1027 †
ω_{CD_2}	—	1116 †	1122 †
ω_{anion1}	2064.6 + 0.1	2067.4 + 0.1	2065.6 + 0.15
ω_{anion2}	2106.3 + 0.2	—	2109.3 + 0.2

† No infrared pressure data are available for the deuterated salt.

TABLE II: Raman and IR frequencies and pressure shifts [4, 5].

the coupling charge transfer band [7, 9]

$$\frac{\omega_R^2 - \omega_{IR}^2}{\omega_R^2} \simeq \lambda \frac{\omega_{CT}^2}{\omega_{CT}^2 - \omega_R^2} \quad (4)$$

(the C=C mode, being an asymmetric combination of A_g molecular modes, couples to the intra-dimer charge transfer [17]). The dominant source of error in this calculation is due to the width of ω_{CT} . The pressure derivative of equation (4),

$$\begin{aligned} \frac{d \ln \lambda}{dP} = & 2 \frac{\omega_{IR}^2}{\omega_R^2 - \omega_{IR}^2} \left[\frac{d \ln \omega_R}{dP} - \frac{d \ln \omega_{IR}}{dP} \right] \\ & + 2 \frac{\omega_R^2}{\omega_{CT}^2 - \omega_R^2} \left[\frac{d \ln \omega_{CT}}{dP} - \frac{d \ln \omega_R}{dP} \right], \end{aligned} \quad (5)$$

has a weaker dependence on the value of ω_{CT} . However we found that the dominant error in (5) arises from the difficulty in determining an accurate pressure dependence of the broad CT band. Constraining the pressure dependence of ω_{CT} to 4 ± 4 %GPa⁻¹ for both b - and c -axes [4], results in an error in the pressure derivative of the coupling constant for the C=C mode of ± 3.5 %GPa⁻¹ for the b -axis and ± 5 %GPa⁻¹ for the c -axis. The error in the pressure derivative of the coupling constant for the C-S mode is larger (8 %GPa⁻¹ for the b -axis and 28 %GPa⁻¹ for the c -axis) because λ_{CS} is so small. The Cu(SCN)₂ anion modes do not exhibit any evidence of electron-phonon coupling, *i.e.* the difference between the infrared and Raman frequencies for the anion modes is accounted for by purely vibrational coupling. The zone center frequency separation, $\Delta\omega_s$, between the symmetric (Raman active) and asymmetric (IR active) combinations of the molecular vibrations, ω_{mol} , is determined by the frequency of the optical branch of the lattice modes, $\omega_{lattice}$ [5, 16],

$$\Delta\omega_s = \frac{\omega_{lattice}^2}{2 \omega_{mol}}. \quad (6)$$

The larger observed $\Delta\omega_s$ for the anion mode in the b -axis response (Table II), for which the lattice mode is stiffer, is a further confirmation of the lattice mode assignment given in [5].

Mode	λ_b	$\frac{d \ln \lambda_b}{dP}$ %GPa ⁻¹	λ_c	$\frac{d \ln \lambda_c}{dP}$ %GPa ⁻¹
ω_{CS}	0.01(1)	47.9	0.02(1)	-11.1
ω_{CC}	0.17(1)	-11.9	0.20(1)	-17.3
ω_{anion1}	0	0	0	0
ω_{anion2}	—	—	0	0

TABLE III: dimensionless electron-phonon coupling constants and their pressure derivatives.

Kozlov *et al.* [17] calculate that the antiphase combination of B_{3g} molecular modes couple to charge transfer perpendicular to the intra-dimer direction. This suggests that the C-S mode couples to intra- not inter-band electronic transitions. It should be noted however, that the electron-phonon coupling constants for the C-S mode have been calculated using the same ω_{CT} as the C=C mode because it is impossible to distinguish the contributions to the IR spectrum from inter- and intra-band transitions.

It has been shown previously [18] that the usual electron-acoustic-phonon interaction mechanism is unable to account for the magnitude of the electron-phonon coupling constant or the large pressure dependence of T_c in the BEDT-TTF superconductors. A further refinement [18] is to include the attractive interaction mediated by the A_g molecular modes, with the total electron phonon coupling constant, λ_{TOT} , given by a Yamaji sum over the individual A_g molecular modes. The energy scale for the interaction is still set by the Debye frequency, Θ [18, 19]. Caulfield *et al.* [2] have previously determined $\Theta \approx 40$ cm⁻¹ by fitting the effective mass dependence of T_c with a linearised Eliashberg equation using an Einstein density of phonon states, $\delta(\Theta)$. High and low temperature specific heat measurements [20, 21] yield values of Θ ranging from 38cm⁻¹ to 140cm⁻¹.

Calculations of λ_{TOT} [18] give values ranging from 0.3-0.45 [22, 23]. Based on the vibrations we sampled, we assume λ_{TOT} to have a pressure dependence similar to that of the strongly coupled C=C mode, *i.e.* of the order of -17 %GPa⁻¹, with an upper limit of -20%GPa⁻¹ used in this calculation. The weak-coupling BCS formula [24] gives a satisfactory explanation of the ambient pressure T_c [7] and accurately describes the effective mass dependence of the superconducting transition temperature [2, 25].

The pressure derivative of the weak-coupling BCS formula provides a convenient parameterization of $\frac{d \ln T_c}{dP}$ in terms of $\frac{d \lambda}{dP}$,

$$\frac{d \ln T_c}{dP} = \frac{d \ln \Theta}{dP} + \frac{1}{(\lambda - \mu^*)^2} \left[\frac{d \lambda}{dP} - \frac{d \mu^*}{dP} \right]. \quad (7)$$

With $\frac{1}{(\lambda-\mu^*)^2} = [\ln(\frac{T_c}{1.13\Theta})]^2$, $\Theta \approx 90 \pm 50 \text{ cm}^{-1}$ [2, 20, 21] and using the average pressure induced stiffening of the Raman active lattice modes $\approx +13 \text{ \%GPa}^{-1}$ [5] for $\frac{d \ln \Theta}{dP}$, the only unknown is the pressure dependence of the Coulomb pseudopotential, $\frac{d\mu^*}{dP}$. Calculations of μ^* [2, 23] indicate a small positive value, a possible indication that direct interactions between the quasiparticles are involved in the pairing. There is also sufficient uncertainty in the parameters necessary to calculate the pressure dependence of the dimer-site Coulomb repulsion [26] that no reliable prediction can be made. We have thus decided to ignore $\frac{d\mu^*}{dP}$ in the above calculation. This gives $\frac{d \ln T_c}{dP} \approx -40 \pm 32 \text{ \%GPa}^{-1}$, which is far from the experimentally observed value of $\frac{d \ln T_c}{dP} \approx -200 \text{ \%GPa}^{-1}$ [2, 3]. As can be seen from (7), Θ directly scales with the pressure dependence of T_c . To obtain the observed rapid fall of T_c with pressure from only the decrease in the electron-phonon coupling constant, requires Θ to be of the order of the C=C mode frequency, $\approx 1500 \text{ cm}^{-1}$. Such a value is utterly inconsistent with the 10 K superconducting temperature and the unconventional isotope shift observed upon carbon substitution [27].

In conclusion we have shown that it is possible to recreate the line shape of the resonance between the central C=C mode and the H (or D) modes in protonated (or deuterated) κ -(BEDT-TTF)₂Cu(SCN)₂. This

was achieved by coupling the strongly infrared active C=C mode to two C-H modes which possessed negligible IR strength of their own. We have also shown that the apparent non-linearity of the pressure dependence of the modes is due to anti-crossing of the mixed modes. We compare high-pressure Raman scattering and IR reflectivity data enabling the pressure dependence of the electron-phonon coupling strength to be evaluated for modes observed in both spectra. Using the weak coupling limit of BCS theory we have been able to compare the pressure dependence of the electron-phonon coupling constant and the pressure dependence of the superconducting transition temperature. This casts considerable doubt on whether this material is a simple BCS superconductor because the characteristic energy of the pairing interaction would have to be of the order of the highest frequency molecular modes, a value inconsistent with the 10 K superconducting transition temperature. This is an indication that electron-electron interaction may be playing a significant role in this material's superconducting mechanism.

The authors thank A.F. Goncharov, V.V. Struzhkin, R.J. Hemley, A. P. Jephcoat and H. Olijnyk for their experimental support and helpful discussions. This work was supported by the EPSRC.

-
- [1] J. Singleton, *Rep. Prog. Phys.* **63**, 1111 (2000).
 [2] J. Caulfield *et al*, *Synth. Metals* **70**, 185 (1995).
 [3] K. Murata *et al*, *Synth. Metals* **27**, A263 (1989).
 [4] A.-K. Klehe *et al*, *J. Phys.: Condens. Matter* **12**, L247 (2000).
 [5] R.D. McDonald *et al*, *J. Phys.: Condens Matter* **13**, L291 (2001).
 [6] K. Kornelsen *et al*, *Solid state commun.* **72**, 475 (1989).
 [7] T. Sugano *et al*, *Phys. Rev. B* **39**, 11387 (1989).
 [8] M.J. Rice, *Solid state commun.* **31**, 93 (1979).
 [9] H. Meneghetti *et al*, *J. Chem. Phys.* **76**, 5785 (1982).
 [10] J.E. Eldridge *et al*, *Spectrochimica Acta* **51A**, 947 (1994).
 [11] K. Kornelsen *et al*, *Solid state commun.* **74**, 501 (1990).
 [12] J.R. Ferraro *et al*, *Solid state commun.* **60**, 917 (1988).
 [13] V.V. Struzhkin *et al*, *Phys. Rev. Lett.* **78**, 4446 (1997).
 [14] A.S. Barker *et al*, *Phys. Rev.* **135**, A1732 (1964).
 [15] R.S. Katiyar *et al*, *Phys. Rev. B* **4**, 2635 (1971).
 [16] R. Zallen, *Phys. Rev. B* **9**, 4485 (1974).
 [17] M.E. Kozlov *et al*, *Synth. Metals* **70**, 1023 (1995).
 [18] K. Yamaji, *Solid state commun.* **61**, 413 (1986).
 [19] J.C.R. Faulhaber *et al*, *Synth. Metals* **60**, 227 (1993).
 [20] B. Andraka *et al*, *Phys. Rev. B* **40**, R11345 (1998).
 [21] N.A. Fortune, *Synth. Metals* **103**, 2080 (1999).
 [22] S. Hill *et al*, *Synth. Metals* **55-57**, 2566 (1993).
 [23] J. Shumway *et al*, *Phys. Rev. B* **53**, 6677 (1995).
 [24] J. Bardeen *et al*, *Phys. Rev.* **108**, 1175 (1957).
 [25] The fact that the weak-coupling BCS expression describes T_c versus m^* well [2] should NOT be taken to imply that κ -(BEDT-TTF)₂Cu(SCN)₂ is a weak-coupling BCS superconductor. The formula is here used as a convenient parameterisation which is known to describe earlier data well [2].
 [26] R.H. McKenzie, *Comments Cond. Matt. Phys.* **18**, 309 (1998).
 [27] J.A. Schlueter *et al*, *Physica C* **351**, 261 (2001).